Earth and Planetary Science Letters 392 (2014) 94–99

Contents lists available at ScienceDirect

Earth and Planetary Science Letters

www.elsevier.com/locate/epsl

Constraining fault friction in oceanic lithosphere using the dip angles of newly-formed faults at outer rises

Timothy J. Craig [a,b,*], Alex Copley [a], Timothy A. Middleton [c]

[a] COMET+, Bullard Laboratories, Department of Earth Sciences, University of Cambridge, Madingley Road, Cambridge, CB3 0EZ, UK
[b] Laboratoire de Géologie, Ecole Normale Supérieure, 24 rue Lhomond, Paris 75231, France
[c] COMET+, Department of Earth Sciences, University of Oxford, South Parks Road, Oxford, OX1 3AN, UK

ARTICLE INFO

Article history:
Received 17 November 2013
Received in revised form 7 February 2014
Accepted 9 February 2014
Available online xxxx
Editor: P. Shearer

Keywords:
fault friction
oceanic lithosphere
rheology
outer rise

ABSTRACT

We investigate the mechanical properties of the oceanic lithosphere using earthquake focal mechanisms from subduction zone outer rises. We study regions where faulting oblique to the pre-existing mid-ocean ridge fabric implies the formation of new faults. The nodal-plane dips of dip-slip earthquakes on these faults are dominantly in the range 30–60°, with a strong peak concentrated around 45°. This distribution is inconsistent with the pattern that would result from high coefficients of friction (e.g. 0.6, equivalent to normal faults forming at 60° and thrust faults at 30°). We instead suggest that the observed distribution of dips implies that faults in the oceanic lithosphere have a low coefficient of friction, due to either low-friction clay minerals formed by hydrothermal alteration at the ridge, or due to an intrinsic level of friction that is lower than that suggested by laboratory studies.

1. Introduction

Early laboratory experiments to determine the coefficient of friction of intact rock (μ — defined as the ratio of the shear and normal stresses on a fault at the point of failure) estimated it to be 0.85 at confining pressures of $\lesssim$200 MPa, and 0.6 at greater confining pressures (Byerlee, 1978). The extrapolation of these values ('Byerlee's Law'), to geological faults, where the effective coefficient of friction is complicated by uncertainties relating to the possible presence of mechanically weak material along active fault planes (e.g., clays, fault rocks; Saffer et al., 2001; Brown et al., 2003; Collettini et al., 2009), and to the influence of pore-fluid on perturbing the effective normal stresses experienced by faults. Studies based on borehole measurements have inferred a range of fault friction values, from ~0.6 (e.g. Zoback and Healy, 1992; Brudy et al., 1997) to $\leqslant$0.3 on mature fault zones (e.g. Lockner et al., 2011). A number of geophysical studies have suggested that mature or reactivated fault systems may be characterised by effective coefficients of friction possibly as low as $\leqslant$0.1 (e.g., Zoback et al., 1987; Lamb, 2006; Herman et al., 2010; Copley et al., 2011; Middleton and Copley, 2013). Given the contrasting views currently held, in this paper we aim to shed further light on the issue of fault friction by examining the earthquakes that occur on newly-formed faults at subduction zone outer rises.

The dip angle at which a given fault plane can be active depends on the orientation and magnitude of the applied stresses, the coefficient of friction of the fault itself (Sibson, 1985), and its tectonic history (which can lead to rotations about horizontal axes; e.g., Jackson and McKenzie, 1983). Hence, if we can isolate a population of newly-formed faults with known dip angles, in regions with a simple and relatively well-understood stress field, we can investigate the frictional properties of these faults. In this paper we use a catalogue of dip-slip earthquakes from subduction zone outer rises. Masson (1991) determined that when the orientation of the pre-existing fabric of the oceanic plate is $\gtrsim$30° different from the local strike of the subduction trench, the bending-related faulting at the outer rise will form new faults parallel to the trench, at an angle to the pre-existing fabric. When the pre-existing fabric is <30° different from the strike of the subduction trench, the bending stresses will reactivate relict structures left from the initial phase of plate formation, rather than breaking new faults. Therefore, by selecting only events with nodal plane strikes parallel to the trench, but oblique to the pre-existing fabric of the downgoing oceanic lithosphere, we can study newly-formed faults, rather than those reactivating the mid-ocean ridge fabric. These faults are the result of extension at the top of the seismogenic layer and compression at the base of the seismogenic layer as the plate bends into the subduction zone (e.g. Chapple and Forsyth, 1979). Where they have been studied in detail, these faults are known to have accumulated relatively little total displacement (rarely more than a few hundred metres of vertical displacement; Masson, 1991; Kobayashi et al., 1998). They will therefore have experienced only

* Corresponding author.
E-mail address: craig@geologie.ens.fr (T.J. Craig).

http://dx.doi.org/10.1016/j.epsl.2014.02.024

minor rotations about horizontal axes and will have an orientation close to that at which they formed. For example, using the expressions of Jackson and McKenzie (1983), we can estimate that faults dipping at 45–60° and spaced ∼10 km apart (e.g. Masson, 1991; Kobayashi et al., 1998) will only rotate by <5° during the accumulation of 500 m of displacement.

In order to investigate the frictional properties of the faults, we must consider the orientation of the local stress field. Here, we make the routine assumption that one of the principal stress directions is vertical, in order to interpret our results in terms of the coefficient of friction on the fault plane (Sibson, 1985; Sibson and Xie, 1998; Collettini and Sibson, 2001). In the case of subduction zone outer rises, the vertical stress axis will be either the maximum principal stress (σ_1) for normal faults, or the minimum principal stress (σ_3) for thrust faults. The assumption of a vertical stress axis is likely to be relatively accurate, because significant deviations are only likely to result from large shear tractions on the base of the lithosphere. Estimates that such tractions are substantially lower than forces being transmitted horizontally through the lithosphere (e.g. Richter and McKenzie, 1978) hence imply that one stress axis will be close to vertical. In the case of the outer rises of subduction zones, there is an additional possibility that one of the principal stresses may be inclined away from the vertical due to the stresses resulting from the bending of the plate into the trench. However, the angle of dip of the oceanic lithosphere in the outer rise and outer-trench slope is typically small (usually $\lesssim$5°). The angle of the plate surface is equivalent to the inclination of the bending-related stresses, and so provides a maximum estimate of the deviation of one of the principal stress axes from vertical. The influence of other forces, especially gravity-driven buoyancy forces, means that the deviation from the vertical of one of the principal stresses will probably be less than this 5° estimate within the outer rise region. We therefore assume that one principal stress is vertical, but note that our interpretations rest upon this assumption. The trench-parallel strikes of earthquake nodal planes in the regions we study imply that the intermediate principal stress is orientated approximately parallel to the trench, and that the final principal stress direction is perpendicular to the trench.

As well as assuming the orientation of the stress field, we also follow previous studies (Sibson, 1985; Sibson and Xie, 1998; Collettini and Sibson, 2001; Middleton and Copley, 2013) in assuming a Mohr–Coulomb yield criterion for the onset of brittle failure. Given that the isotropic part of the stress tensor is compressional, we can discount non-linear relations between the shear and normal stresses at small or negative values of the normal stress (e.g., Griffiths failure). Whilst numerous other formulations for the yield criteria exist, the Mohr–Coulomb criterion remains the most appropriate when assessing the onset of brittle, seismogenic, behaviour at the stress magnitudes relevant to this tectonic setting ($\lesssim$300 MPa; e.g., Craig et al., in press). For example, the commonly-used von Mises failure criterion relates to plastic deformation at high stresses, rather than brittle failure in earthquakes.

2. Observations of earthquake nodal-plane dips

A recent global study (Craig et al., in press) compiled a catalogue of outer-rise earthquakes with well-constrained source parameters derived from the modelling of seismic body-waveforms (discussed in more detail below). Here, we take a subset of earthquakes from this catalogue, restricted to regions where the pre-existing oceanic fabric (parallel to the ridge at the time the crust was formed, and so parallel to isochrons) is oblique to the strike of the trench (see Fig. 1). Earthquakes from the catalogue of Craig et al. (in press) with well-determined focal mechanisms that show nodal-plane orientations oblique to the local strike of the trench, suggesting that the bending-related stresses are not dominant, are also excluded, leaving a dataset of earthquakes striking parallel or sub-parallel to the local trench, and oblique to the pre-existing oceanic fabric. These earthquakes (Fig. 1) are therefore likely to represent slip on newly-formed faults in oceanic lithosphere, being formed in close proximity to the subduction zone as a response to the bending of the plate (Masson, 1991).

The earthquake focal mechanisms presented in Fig. 1 have been determined by the inversion of long-period *P*- and *SH*-bodywaves (Craig et al., in press, and references therein), or, for some of the larger earthquakes, by the inversion of the *W*-phase (e.g. Lay et al., 2010). The body-waveform modelling was undertaken using routine techniques described in detail elsewhere (e.g., Taymaz et al., 1991; Craig et al., in press). The accuracy of the focal mechanisms is dependent on the quality of the available data, the coverage of the focal sphere, and the complexity of the earthquake, but the likely errors in the nodal-plane dip estimates are typically ±5–10° (e.g. Molnar and Lyon-Caen, 1989; Taymaz et al., 1991). Fig. 2 presents a set of dip sensitivity tests for six outer-rise normal-faulting earthquakes: one from the Philippines, two from the Japan trench east of Honshu, and three from the Tonga–Fiji subduction zone. These events are representative of the others shown in Fig. 1. In these tests, the dip is fixed at 1° increments, and the best-fitting source mechanism then calculated by least-squares inversion of the waveform data with all other source parameters (strike, rake, depth, moment and source-time function) free to vary. The shapes of the misfit curves in Fig. 2 give a good indication of how well constrained the dips of the nodal planes are, and dip variations of more than 5–10° from the best fit result in a significantly worse fit to the data. The accuracy of focal mechanisms determined in this manner is confirmed by comparison in continental settings with independent geodetically-derived solutions (e.g. Copley et al., 2012; Devlin et al., 2012). In the absence of clear evidence of rupture propagation from directionality in the waveforms, seismologically-derived focal mechanisms are unable to distinguish between the actual fault plane and its auxiliary, leading to two minima in the misfit curve, corresponding to these two possible fault planes (indicated by the coloured circles in Fig. 2). Further uncertainty in dip determination may arise from unmodelled complications in the near-source velocity structure. However, tests to determine the effect of minor variations in structure near the source show that it has little effect on the geometry of the focal mechanism, and mainly influences the source depth (Nelson et al., 1987; Middleton and Copley, 2013).

Fig. 3 presents histograms showing the dip angles of the nodal planes from the earthquakes shown in Fig. 1. Given the uncertainty over which nodal plane is the actual fault plane, both planes from all earthquakes in Fig. 1 are used in plotting the fault-dip populations in Fig. 3. Both normal- and thrust-faulting earthquake populations show a range in dip angles concentrated between 30 and 60°, with a small number of outliers at higher/lower dip angles. This range is consistent with the findings of earlier focal mechanism studies of dip-slip earthquakes from continental regions (e.g. Jackson and White, 1989; Thatcher and Hill, 1991; Sibson and Xie, 1998; Collettini and Sibson, 2001). In contrast with an earlier compilation of outer-rise earthquake dips using a smaller catalogue (Thatcher and Hill, 1995), which showed a peak at 55 ± 6°, the normal-fault population in our compilation (Fig. 3B) shows a notable maximum at 45 ± 5°. The difference between these two studies probably results from the larger dataset used in our compilation, and our exclusion of events from outer rise regions where earthquakes are likely to have occurred on reactivated pre-existing structures. Given that the earthquakes we study are generally close to pure dip-slip (Fig. 1), the

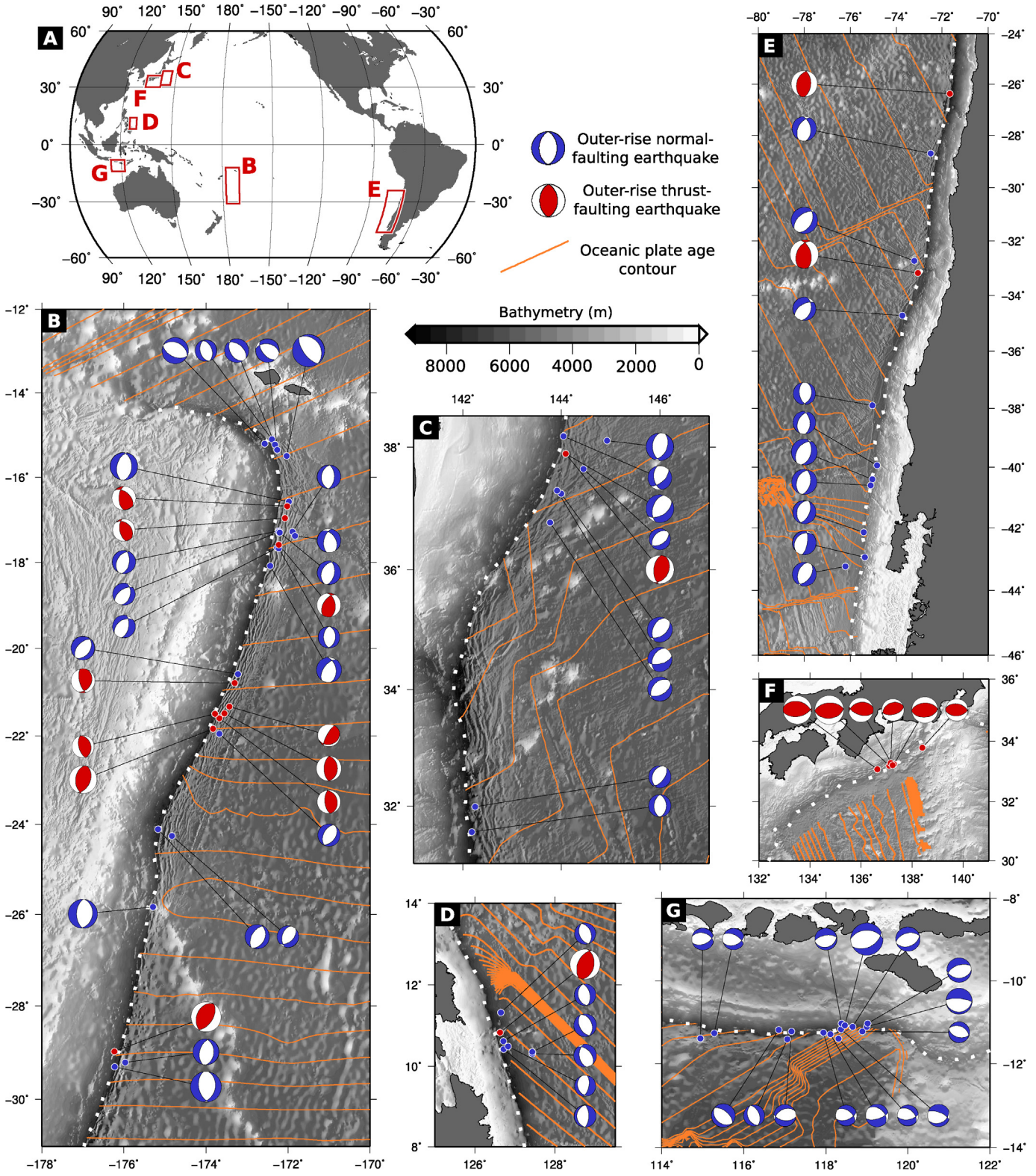

Fig. 1. Maps of regions where outer-rise earthquakes are occurring on faults oblique to the local oceanic fabric. (A) Regional location map. (B) The Tonga–Fiji subduction zone. (C) East of Honshu. (D) The Philippines subduction zone. (E) The Chilean subduction zone. (F) South of Shikoku. (G) Sumba. In each case, outer-rise earthquakes with well-constrained source parameters (Craig et al., in press, and references therein) are plotted, along with ocean age contours from Muller et al. (2008) at 1 Myr intervals, and bathymetry from Becker et al. (2009).

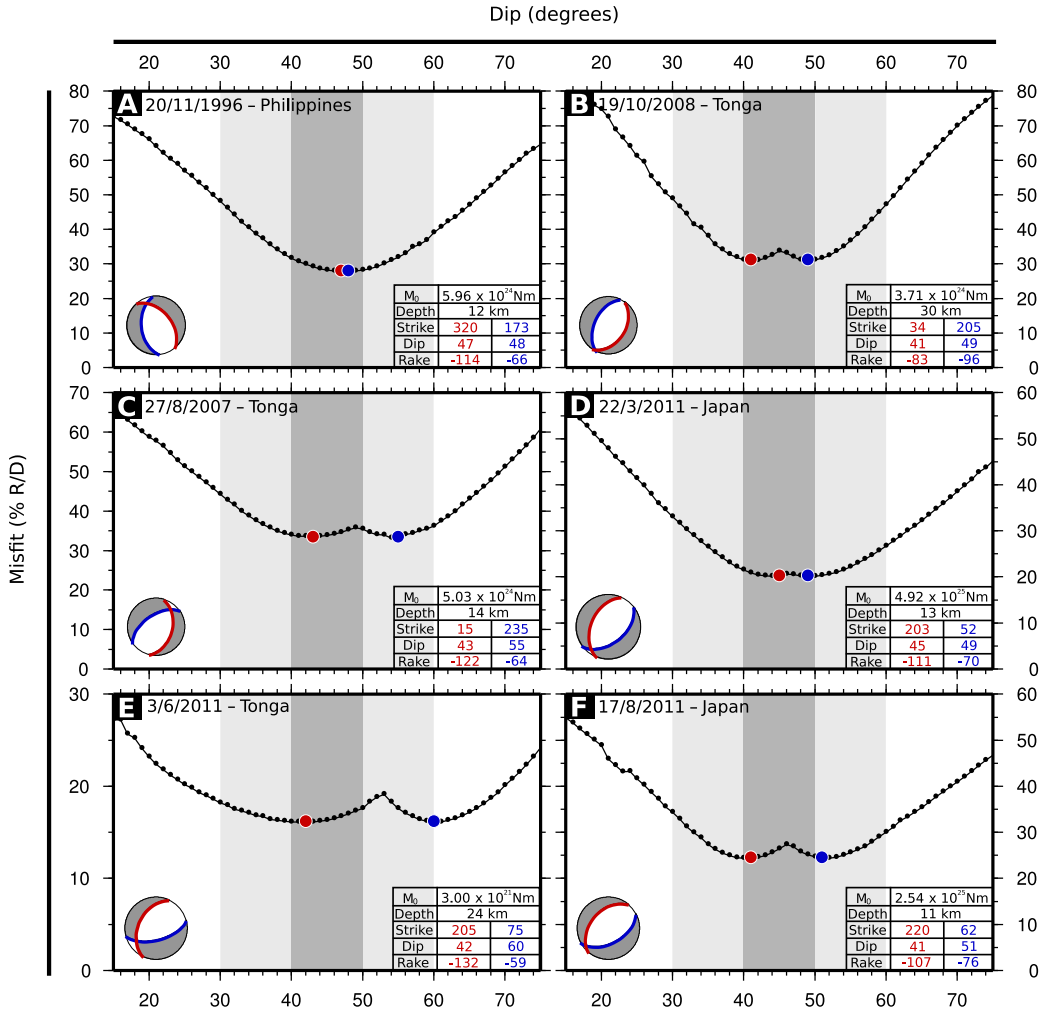

Fig. 2. Sensitivity tests for seismologically determined estimates of dip. Misfit curves are calculated by fixing the dip at 1° increments, and inverting for a best-fit solution with all other parameters free. $\%R/D$ is a measure of the residual between the data and synthetics. The two minima correspond to the two nodal planes of the overall minimum mistfit solution (indicated by the coloured circles, matched with their respective planes in the table and on the focal mechanism). The parameters given in the tables are the minimum misfit solutions for each nodal plane.

concentration around 45° must reflect the geometries of the actual fault planes and their auxiliaries, rather than the auxiliary planes of higher- or lower-angled events (Fig. 2), which for pure dip-slip events would plot away from 45°. The population of thrust-faulting earthquakes (Fig. 3C) is too small for any clear trends to emerge, and is not the subject of further analysis in this study. We instead focus on the dip distribution of normal-faulting earthquakes.

The interpretation of nodal-plane dip distributions is complicated by the fact that only half of the data points represent real fault-plane dips (see discussions in Thatcher and Hill (1991) and Middleton and Copley (2013)). However, given our estimated errors in the nodal plane dip determinations, and the fact that for pure dip-slip events only faults dipping at 45° can have fault or auxiliary planes with this dip, we can conclude that the distribution in Fig. 3B represents the rupture of faults with dips at, or close to, 45°, in order to reproduce the observed peak. This distribution of earthquake dips is consistent with the sparse available estimates of outer rise fault dips based on morphological observations. For example, bathymetric estimates of the dip of surficial fault escarpments east of Honshu in the Japan trench give an average dip of ∼38° (Kobayashi et al., 1998). However, due to the difficulty of imaging basement faults in oceanic lithosphere, no other estimates are available for comparison with our earthquake results.

3. Implications for fault friction

Previous compilations of continental dip-slip earthquakes have suggested that normal-fault systems form at ∼60°, undergo rotation about a horizontal axis during the accumulation of slip on the fault, and then become inactive when the dip reaches ∼30°. At this point, it is thought to become more favourable to break a new high-angle fault than to continue to move a fault at low dip angles (Thatcher and Hill, 1991; Sibson and Xie, 1998; Collettini and Sibson, 2001), although Thatcher and Hill (1991) suggested that stress transfer from the ductile lithosphere could also play a role. For a normal fault initiating at a dip of 60° to be rotated to 45° requires an extension factor (β — McKenzie, 1978) of ∼1.2 (using the expressions of Jackson and McKenzie, 1983). Although the top surface of the plate at the outer rise is in extension due to the bending into the subduction zone, the overall strain is low (average extension factors over the bending region of <1.05, from simple kinematic calculations and observations of fault-offsets; Kobayashi et al., 1998; Craig et al., in press). Therefore, it is unlikely that the faults at ∼45° that broke in the earthquakes we have studied have been rotated from 60° to this dip. The dip distribution we have observed is therefore inconsistent with the normal faults initiating at 60°, as implied by Byerlee's Law, which in the absence of significant horizontal-axis rotations

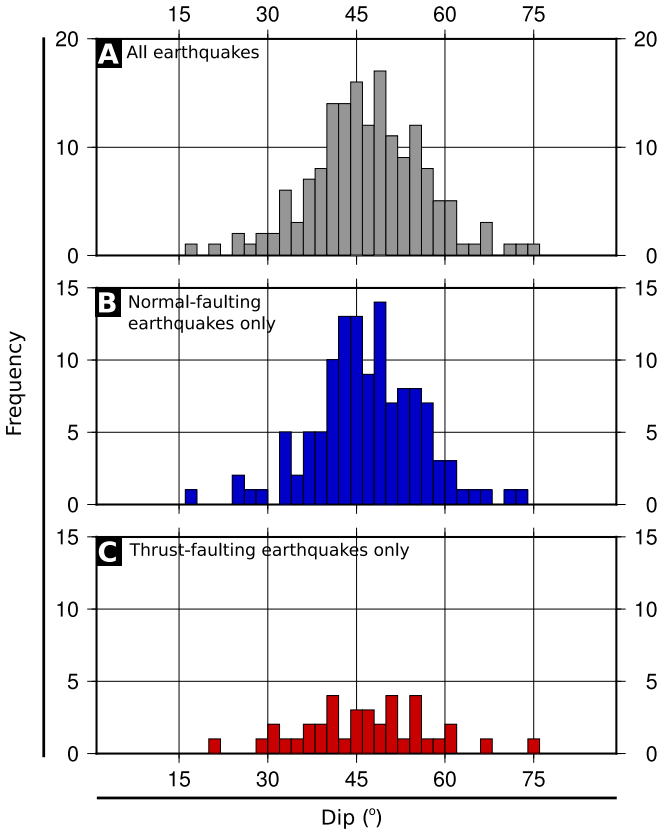

Fig. 3. Nodal plane dip populations. (A) For all outer rise earthquakes in regions where new faults are forming at an angle to the pre-existing oceanic fabric (81 earthquakes). (B) Normal-faulting earthquakes only (61 earthquakes). (C) Thrust-faulting earthquakes only (20 earthquakes). For all earthquakes, both nodal planes are plotted.

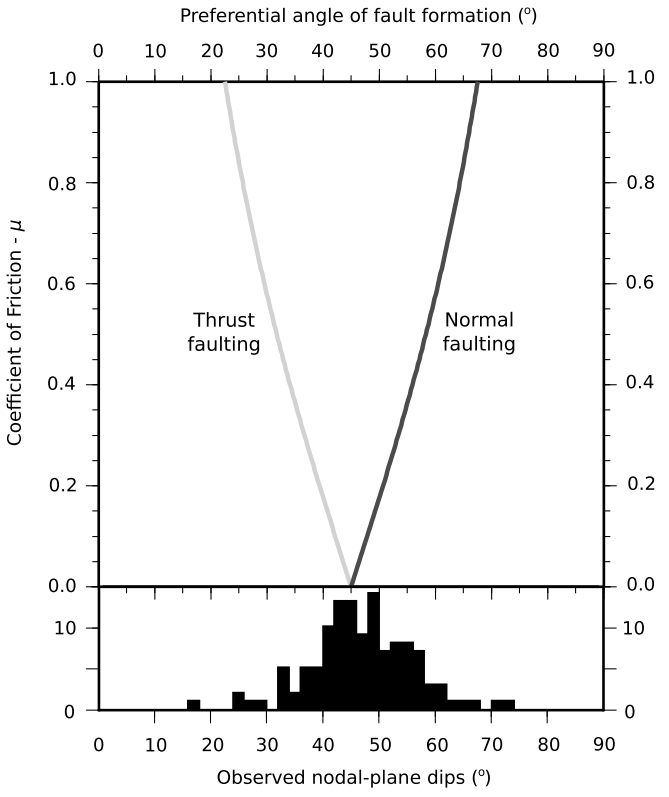

Fig. 4. Optimum angles of fault-formation as a function of the coefficient of friction. Lower panel reproduces the histogram from Fig. 3B for observed nodal plane dips of outer rise normal-faulting earthquakes.

would result in twin peaks at 60 and 30° in Fig. 3 (representing the fault and auxiliary planes).

In the case of the outer rise, Thatcher and Hill (1995) suggested that the bending of the lithosphere into the trench could result in the rotation of outer rise faults about a horizontal axis. However, this rotation is typically $\lesssim$5° over the region failing in earthquakes, as indicated by the change in dip of the seafloor, which implies that the passive rotation of the faults due to this bending is minor. Additionally, it is likely that many of the faults form within the trench-slope region, rather than at the crest of the outer rise, so will have experienced less rotation due to the bending of the lithosphere than implied by the dip of the seafloor.

Fig. 4 shows theoretical values for the optimum angle of fault formation as a function of the coefficient of friction (Turcotte and Schubert, 2002). These curves show the angle at which, for a given coefficient of friction, the ratio of maximum to minimum principal stress required to cause faulting ($\frac{\sigma_1}{\sigma_3}$) is the smallest. Hence, as the plate bends into the trench, and σ_1 gradually increases as the bending stresses increase, new faults should form at the optimum orientation for faulting at the lowest possible σ_1. A coefficient of friction of 0.6 (Byerlee's Law) would indicate the formation of normal faults at ~60°. The observed concentration of nodal planes close to 45° instead suggests a much lower coefficient of friction. Given the uncertainties of 5–10° in dip estimates, we can constrain the coefficient of friction to be less than ~0.3, with an unconstrained lower bound due to the possibility of all the faults dipping at 45° and the spread in the histogram being due to errors in the mechanism determinations.

Previous observations of faults with low coefficients of friction have suggested that this results from the presence of weak fault-rocks along the fault plane, due to either mechanical or chemical alteration of the material through which the fault passes (e.g., Collettini, 2011; Lockner et al., 2011). Outer-rise faults have been suggested to act as conduits for the penetration of significant volumes of water deep into the oceanic crust and mantle (Ranero et al., 2003), which would probably result in mineralogical alteration along the penetration pathway, and formation of weak hydrated mineral phases along the fault plane, lowering its coefficient of friction. However, this process would be unable to affect the initial angle of fault formation, only the mechanical properties of existing faults. We must also consider the effect of variations in the pore-fluid pressure on our results. In the case where the coefficient of friction is independent of the normal stress, changes in the pore-fluid pressure are unable to change the optimum angle of failure, only the stress level at which this failure occurs (e.g., Middleton and Copley, 2013). Hence, whilst the pore-fluid pressure in subduction zone outer rises is unknown, it does not affect our conclusions.

There are two potential explanations for the low coefficient of friction implied by the earthquake nodal plane dips. First, the hydrothermal alteration of the crust during formation at mid-ocean ridges (VanTongeren et al., 2008; Maclennan et al., 2005) could have left a network of weak minerals (e.g. talc, serpentine) that could lower the coefficient of friction of the oceanic crust along planes in many possible orientations, and unrelated to the spreading fabric. This hypothesis requires such hydrothermal alteration to be pervasive throughout the uppermost oceanic lithosphere. New faults forming within the oceanic crust could therefore be doing so in low-friction rocks, resulting in the formation of fault planes at angles close to 45°. The growth of these faults into the upper mantle as they accumulate displacement could then result in the entire part of the plate in tension breaking along faults dipping at ~45°. Alternatively, under geological conditions, the oceanic lithosphere may have an intrinsically low coefficient of friction, inaccurately represented by experimental studies at different pressures,

temperatures, fluid compositions, and fluid pressures. With the information we have available, we are not able to distinguish between these possibilities, and are only able to conclude that the coefficient of friction of oceanic crust in orientations not related to the pre-existing spreading fabric is low ($\lesssim$0.3). It is interesting to note that similar studies of earthquake nodal-plane dips from normal-faulting earthquakes occurring at mid-ocean ridges also show a strong clustering at $\sim$45° (Thatcher and Hill, 1995), perhaps indicating that the rheological control on the angles of fault formation in both settings is the same.

4. Conclusions

We have presented a dataset of earthquake nodal-plane dip angles for newly formed faults at the outer rises of subduction zones. The observed concentration of the distribution around 45° is consistent with a scenario in which oceanic lithosphere is either pervasively weak, and governed by a low coefficient of friction, or permeated by low-friction minerals formed during hydrothermal alteration at the mid-ocean ridges.

Acknowledgements

We thank Simon Lamb and one anonymous reviewer for their helpful comments. This work forms part of the NERC- and ESRC-funded project 'Earthquakes without Frontiers'. Figures were produced using the Generic Mapping Tools (GMT) software.

References

Becker, J.J., Sandwell, D.T., Smith, W.H.F., Braud, J., Binder, B., Depner, J., Fabre, D., Factor, J., Ingalls, S., Kim, S.-H., Ladner, R., Marks, K., Nelson, S., Pharaoh, A., Sharman, G., Trimmer, R., VonRosenburg, J., Wallace, G., Weatherall, P., 2009. Global bathymetry and elevation data at 30 arc seconds resolution: SRTM30PLUS. Mar. Geod. 32 (4), 355–371.

Brown, K.M., Kopf, A., Underwood, M.B., Weinberger, J.L., 2003. Compositional and fluid pressure controls on the state of stress on the Nankai subduction thrust: A weak plate boundary. Earth Planet. Sci. Lett. 214, 589–603.

Brudy, M., Zoback, M.D., Fuchs, K., Rummel, F., Baumgartner, J., 1997. Estimation of the complete stress tensor to 8 km depth in the KTB scientific drill holes: Implications for crustal strength. J. Geophys. Res. 102, 18453–18475.

Byerlee, J., 1978. Friction of rocks. Pure Appl. Geophys. 116, 615–626.

Chapple, W.M., Forsyth, D.W., 1979. Earthquakes and bending of plates and trenches. J. Geophys. Res. 84, 6729–6749.

Collettini, C., 2011. The mechanical paradox of low-angle normal-faults: current understanding and open questions. Tectonophysics 510, 253–268. http://dx.doi.org/10.1016/j.tecto.2011.07.015.

Collettini, C., Sibson, R.H., 2001. Normal faults, normal friction?. Geology 29, 927–930.

Collettini, C., Niemeijer, A., Viti, C., Marone, C., 2009. Fault zone fabric and fault weakness. Nature 462, 907–911.

Copley, A., Avouac, J.-P., Hollingsworth, J., Leprince, S., 2011. The 2001 M_w 7.6 Bhuj earthquake, low fault friction, and the crustal support of plate driving forces in India. J. Geophys. Res. 116. http://dx.doi.org/10.1029/2010JB008137.

Copley, A., Hollingsworth, J., Bergman, E., 2012. Constraints on fault and lithosphere rheology from the coseismic slip and postseismic afterslip of the 2006 M_W 7/0 Mozambique earthquake. J. Geophys. Res. 117. http://dx.doi.org/10.1029/2011JB008580.

Craig, T.J., Copley, A., Jackson, J., in press. A reassessment of outer-rise seismicity and its implications for the mechanics of oceanic lithosphere. Geophys. J. Int. http://dx.doi.org/10.1093/gji/ggu013.

Devlin, S., Isacks, B.L., Pritchard, M.E., Barnhart, W.D., Lohman, R.B., 2012. Depths and focal mechanisms of crustal earthquakes in the central Andes determined from teleseismic waveform analysis and InSAR. Tectonics 31. http://dx.doi.org/10.1029/2011TC002914.

Herman, F., Copeland, P., Avouac, J.-P., Bollinger, L., Mahéo, G., Le Fort, P., Rai, S., Foster, D., Pêcher, A., Stüwe, K., Henry, P., 2010. Exhumation, crustal deformation, and thermal structure of the Nepal Himalaya derived from the inversion of thermochronological and thermobarometric data and modeling of the topography. J. Geophys. Res. 115. http://dx.doi.org/10.1029/2008JB006126.

Jackson, J., McKenzie, D., 1983. The geometrical evolution of normal fault systems. J. Struct. Geol. 5, 471–472.

Jackson, J.A., White, N.J., 1989. Normal faulting in the upper continental crust: observations from regions of active extension. J. Struct. Geol. 11, 15–36.

Kobayashi, K., Nakanishi, M., Tamaki, K., Ogawa, Y., 1998. Outer slope faulting associated with the western Kurils and Japan trenches. Geophys. J. Int. 134, 356–372.

Lamb, S., 2006. Shear stresses on megathrusts: Implications for mountain building behind subduction zones. J. Geophys. Res. 111. http://dx.doi.org/10.1029/2005JB003916.

Lay, T., Ammon, C.J., Kanamori, H., Rivera, L., Koper, K.D., Hutko, A.R., 2010. The 2009 Samoa–Tonga great earthquake triggered doublet. Nature 466. http://dx.doi.org/10.1038/nature09214.

Lockner, D.A., Marrow, C., Moore, D., Hickman, S., 2011. Low strength of deep San Andreas fault gouge from SAFOD core. Nature 472, 82–86. http://dx.doi.org/10.1038/nature09927.

Maclennan, J., Hulme, T., Singh, S.C., 2005. Cooling of the lower oceanic crust. Geology 33. http://dx.doi.org/10.1130/G21207.1.

Masson, D.G., 1991. Fault patterns at outer trench walls. Mar. Geophys. Res., 209–225.

McKenzie, D., 1978. Some remarks on the development of sedimentary basins. Earth Planet. Sci. Lett. 40, 25–32.

Middleton, T.A., Copley, A., 2013. Constraining fault friction by re-examining earthquake nodal plane dips. Geophys. J. Int. 196, 671–680. http://dx.doi.org/10.1093/gji/ggt427.

Molnar, P., Lyon-Caen, H., 1989. Fault plane solutions of earthquakes and active tectonics of the Tibetan Plateau and its margins. Geophys. J. Int. 99, 123–153.

Muller, R.D., Sdrolias, M., Gaina, C., Roest, W.R., 2008. Age, spreading rates, and spreading asymmetry of the world's ocean crust. Geochem. Geophys. Geosyst. 9. http://dx.doi.org/10.1029/2007GC001743.

Nelson, M.R., McCaffery, R., Molnar, P., 1987. Source parameters for 11 earthquake in the Tien Shan, Central Asia, determined by *P* and *SH* waveform inversion. J. Geophys. Res. 92, 12629–12648.

Ranero, C.R., Phipps Morgan, J., McIntosh, K., Reichert, C., 2003. Bending-related faulting and mantle serpentinization at the Middle America trench. Nature 425, 367–374.

Richter, F., McKenzie, D., 1978. Simple plate models for mantle convection. J. Geophys. 44, 441–471.

Saffer, D.M., Fyre, K.M., Marone, C., Mair, K., 2001. Laboratory results indicating complex and potentially unstable frictional behaviour of smectite clay. Geophys. Res. Lett. 28, 2297–2300.

Sibson, R.H., 1985. A note on fault reactivation. J. Struct. Geol. 7, 751–754.

Sibson, R.H., Xie, G., 1998. Dip range for intracontinental reverse fault ruptures: Truth not stranger than friction. Bull. Seismol. Soc. Am. 88, 1014–1022.

Taymaz, T., Jackson, J., McKenzie, D., 1991. Active tectonics of the north and central Aegean Sea. Geophys. J. Int. 106, 433–490.

Thatcher, W., Hill, D.P., 1991. Fault orientation in extensional and conjugate strike-slip environments and their implications. Geology 19, 1116–1120.

Thatcher, W., Hill, D.P., 1995. A simple model for the fault-generated morphology of slow-spreading mid-oceanic ridges. J. Geophys. Res. 100, 561–570.

Turcotte, D., Schubert, G., 2002. Geodynamics. Cambridge University Press.

VanTongeren, J.A., Kelemen, P.B., Hanghøj, K., 2008. Cooling rates in the lower crust of the Oman ophiolite: Ca in olivine, revisited. Earth Planet. Sci. Lett. 267, 69–82. http://dx.doi.org/10.1016/j.epsl.2007.11.034.

Zoback, M.D., Healy, J.H., 1992. In situ stress measurements to 3.5 km depth in the Cajon Pass Scientific Research Borehole: Implications for the mechanics of crustal faulting. J. Geophys. Res. 97, 5039–5057.

Zoback, M.D., Zoback, M.L., Mount, V.S., Suppe, J., Eaton, J.P., Healy, J.H., Oppenheimer, D., Reasenberg, P., Jones, L., Raleigh, C.B., Wong, I.G., Scotti, O., Wentworth, C., 1987. New evidence on the state of stress of the San Andreas fault system. Science 238, 1105–1111.